

# Revealing the Cluster-Cloud and Its Role in Nanocrystallization

Biao Jin, Yanming Wang, Zhaoming Liu, Arthur France-Lanord, Jeffrey C. Grossman, Chuanhong Jin,\* and Ruikang Tang\*

Elucidating the early stages of crystallization from supersaturated solutions is of critical importance, but remains a great challenge. An in situ liquid cell transmission electron microscopy study reveals an intermediate state of condensed atomic clusters during Pd and Au crystallizations, which is named a “cluster-cloud.” It is found that nucleation is initiated by the collapse of a cluster-cloud, first forming a nanoparticle. The subsequent particle maturation proceeds via multiple out-and-in relaxations of the cluster-cloud to improve crystallinity: from a poorly crystallized phase, the particle evolves into a well-defined single-crystal phase. Both experimental investigations and atomistic simulations suggest that the cluster-cloud-mediated nanocrystallization involves an order–disorder phase separation and reconstruction, which is energetically favored compared to local rearrangements within the particle. This finding grants new insights into nanocrystallization mechanisms, and provides useful information for the improvement of synthesis pathways of nanocrystals.

Nanocrystals have received great attentions due to their many applications in catalysis, biomedicine, sensing, and so forth.<sup>[1]</sup> An in-depth understanding of crystallization processes is key to nanomaterials design and preparation.<sup>[2]</sup> Despite intensive studies about classical or nonclassical crystallization theories,<sup>[3]</sup> the current knowledge of early stages of crystallization is very limited. For example, the pathway from the early phase separation of atoms, ions, or molecules from solutions to the nanoparticle formation is still unclear.<sup>[4]</sup> Toward filling this gap, multiple-step models have been recently proposed,<sup>[5]</sup>

which emphasize the presences of several intermediate states prior to nucleation, such as amorphous precursors,<sup>[5c,6]</sup> magic-size clusters,<sup>[7]</sup> condensed liquid phase,<sup>[8]</sup> prenucleation clusters,<sup>[9]</sup> etc. Although it is suggested that the energetic barrier for multistep nucleation via intermediate states is lower than that expected in a classical nucleation picture,<sup>[10]</sup> debates remain due to the lack of direct experimental evidence for early crystallization.<sup>[4b,5a,c,7,11]</sup>

The diversity and details of nonclassical nucleation and crystallization pathways (e.g., multistep nucleation process and amorphous precursor phase) of nanocrystals have been revealed at the nanoscale using liquid-cell transmission electron microscopy (LC-TEM).<sup>[5a,6b]</sup> The technical advancement of LC-TEM consists in its capability of tracking ultrasmall and metastable objects in solution,<sup>[5a,6b]</sup> making it a


powerful tool to analyze liquid specimens and achieving in situ visualization with high spatial resolution.<sup>[12]</sup> Motivated by these recent advancements, we presently explore details in nanocrystallization<sup>[3]</sup> to achieve a full mechanistic understanding. In this communication, we analyze Pd and Au crystallizations using LC-TEM, and unravel an alternative nanocrystallization process involving an intermediate state which we dub cluster-cloud. This new phase plays a vital role in nucleation and particle structural evolution: the initial nucleation results from a sudden collapse of the cluster-cloud; and the subsequent particle maturation undergoes via the cluster-cloud mediated out-and-in relaxations. This discovery underscores the diversity and complexity of crystallization pathways and improves our current knowledge by providing a more comprehensive picture of nanocrystal formation.

For the in situ LC-TEM observations of Pd and Au crystallization, solutions containing 400 nL 10.0 mM Na<sub>2</sub>PdCl<sub>4</sub> and HAuCl<sub>4</sub>, respectively, were prepared in the liquid-cells. High-energy electrons from TEM generated solvated electrons to reduce solution Pd<sup>2+</sup><sup>[13]</sup> and Au<sup>3+</sup><sup>[14]</sup> to Pd and Au atoms, respectively (see Method in the Supporting Information for details). The time sequenced TEM images (**Figure 1a**) show the prenucleation and nucleation of Pd. Similar to Mirsaidov's observation of metal-rich liquid phase,<sup>[5a]</sup> a dark region formed (0 s), corresponding to the concentration of the reduced Pd atoms from solution. This irregular region was flexible with a cloud-like behavior (18 s). It is noteworthy that instead of a random assembly of atoms, this cloud consisted of several

B. Jin, Dr. Z. Liu, Prof. R. Tang  
Department of Chemistry  
Zhejiang University  
Hangzhou, Zhejiang 310027, China  
E-mail: rtang@zju.edu.cn

Dr. Y. Wang, Dr. A. France-Lanord, Prof. J. C. Grossman  
Department of Materials Science and Engineering  
Massachusetts Institute of Technology  
77 Massachusetts Avenue, Cambridge, MA 02139, USA

Prof. C. Jin, Prof. R. Tang  
State Key Laboratory of Silicon Materials  
School of Materials Science and Engineering  
Zhejiang University  
Hangzhou, Zhejiang 310027, China  
E-mail: chhjin@zju.edu.cn

 The ORCID identification number(s) for the author(s) of this article can be found under <https://doi.org/10.1002/adma.201808225>.

DOI: 10.1002/adma.201808225

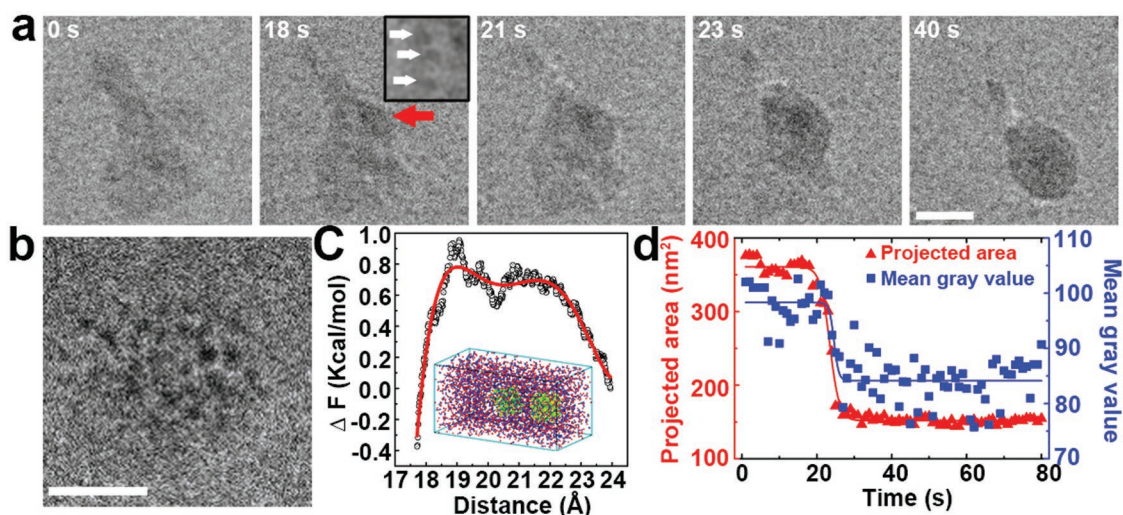


**Figure 1.** Cluster-cloud mediated Pd nanocrystal prenucleation and nucleation processes. a) Sequential TEM images, showing the cluster-cloud transforming into a nanoparticle. Scale bar, 10 nm. b) The early stage structure before the cluster-cloud formation, showing the existence of nanoclusters. Scale bar, 5 nm. c) The free energy change ( $\Delta F$ ) as a function of interparticle distance during the coalescence of two Pd nanoclusters, showing that these clusters could be stabilized by water molecules. d) Projected area and mean gray value as a function of time during the nanoparticle formation process.

$\approx 1.0$  nm ultrasmall clusters (Figure 1b), similar in size with the prenucleation clusters reported by Cölfen and co-workers.<sup>[9a]</sup> According to our ex situ examination (Figure S1, Supporting Information), no significant crystalline characteristics were found in these clusters, implying an amorphous state of the sample. It has been documented that amorphous Pd nanoclusters can be highly hydrated and stabilized by water.<sup>[15]</sup> Accordingly, using steered molecular dynamics (SMD) simulation,<sup>[16]</sup> we showed that a free energy barrier should be overcome for any coalescence of the Pd nanoclusters under aqueous condition (Figure 1c). At 18 s (Figure 1a), a region with high local contrast (noted by a red arrow) appeared within the cluster-cloud, which could be regarded as the nucleus. Then the initial nucleation occurred through a sudden collapse of the cluster-cloud, forming nanoparticle (23 and 40 s in Figure 1a). This transition could also be understood quantitatively by gray and projected area analyses (Figure 1d), showing an abrupt condensation of matter at 18–23 s. More details about this process can be found in Movie S1 in the Supporting Information. The examinations showed that each Pd nanoparticle produced by the condensation was poorly crystallized (Figure S2, Supporting Information).

The condensation of cluster-cloud was frequently observed (Figure S3, Supporting Information) in our experiments. Using dynamic light scattering (DLS), we characterized the change in size of Pd nanoparticles in a mixed solution of  $\text{Na}_2\text{PdCl}_4$  and  $\text{NaBH}_4$  (Figure S4, Supporting Information) during the early crystallization period. The fluctuation of the nanoparticles size in the bulk solution might be associated with the cluster-cloud mediated nucleation observed by LC-TEM.

Interestingly and importantly, this cluster-cloud intermediate phase was also observed in the subsequent nanoparticle maturation stage (Figure S5, Supporting Information), which cannot be rationalized with established understandings.<sup>[3a]</sup> **Figure 2** summarizes our analyses of a typical process (Movie S2, Supporting Information). It showed that some loose matter can be continuously expelled from the particle (the period of 3–23 s) after the condensation (Figure 2a). These expelled chunks did not dissolve in solution; instead, they formed clouds around the core-host nanoparticle (named as “out”). During the “out” process, the particle core kept shrinking with the cloud expanding (Figure 2b), which is evidence of a transfer of matter from the particle to the cloud. The primary component of the remaining particle was determined to be crystallized Pd, while

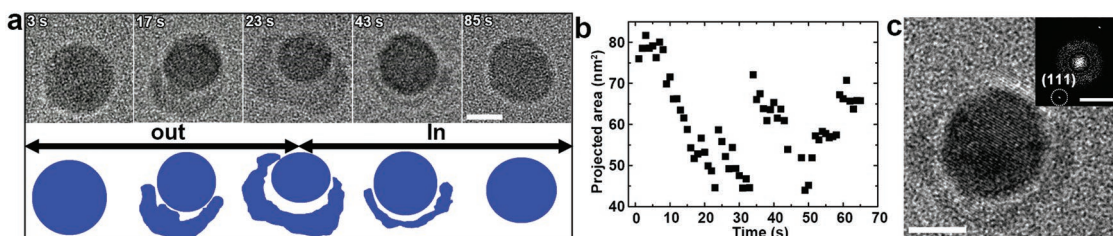


**Figure 2.** The cluster-cloud mediated Pd nanocrystal relaxation process. a) Sequential TEM images and corresponding schematic, showing the typical cluster-cloud relaxation mechanism of “out” and “in” processes. b) The “core” projected area changes of Pd nanocrystal during the relaxation process, showing multiple out-and-in relaxations. c) The TEM image shows the internally ordered Pd nanocrystal. Scale bar, 5 nm. Inset in “c”: the corresponding FFT image where the scale bar is 5  $1/\text{nm}$ .

the cloud consisted of amorphous Pd nanoclusters (Figure 2c). In this state, the newly resulted cloud is exactly comparable to the original cluster-cloud prior to the nucleation. This particle-cloud structure was found to be metastable, since the cloud phase could be gradually adsorbed by the core particle with time (23–85 s) (named as “in”). During the “in” process, the particle expanded while the size of the cloud decreased (Figure 2b), indicating that the matter returned from cloud to particle. The “out” and “in” processes constituted the nanoparticle maturation, which is defined as out-and-in relaxation.

In fact, the out-and-in relaxation was not a rare or exceptional event under LC-TEM; on the contrary, this phenomenon may occur frequently. More cases are provided in Figures S6–S9 in the Supporting Information. In Figure S8b (Supporting Information), the cluster-cloud relaxation was also observed around relatively large particles. But it should also be mentioned that not every nanocrystal experienced the out-and-in relaxation in our in situ LC-TEM observation period. Furthermore, this process is not only specific to the nanocrystallization of Pd, but also appears in the Au system (Figure S10, Supporting Information). The above abundant experimental data suggests the universality of the cluster-cloud configuration and the associated out-and-in relaxation. Then, a rising question is, how can we understand this relaxation process in nanocrystallization? Taking the advantage of LC-TEM, we examined the crystallinity change of the particle using high-resolution images combined with fast Fourier transform (FFT)<sup>[17]</sup> (Figure 3a; Movie S3, Supporting Information). Figure 3a shows that at 6 s, there were different lattice orientations inside the Pd nanoparticle, a clear indicator of polycrystallinity. During the matter ejection

(“out,” 126 s), the particle core became smaller in size but its crystallinity significantly improved, as only one lattice orientation was identified. This crystalline order improvement could be preserved during the “in” process (203 s). Ex situ high resolution TEM confirmed this transition state during Pd nanocrystal maturation, showing that the structure of a well-crystallized particle was formed while the disordered amorphous phase was being ejected as cloud (Figure 3b). We suggest that both “out” and “in” processes can improve the crystallinity as well as the orientation homogenization. In fact, the originally resulted poorly crystallized nanoparticle can become a single crystal after undergoing several cycles of out-and-in relaxation. A quantitative measurement of the crystalline ordering change during particle relaxation is demonstrated by using the Herman's order parameter ( $f$ ) (Figure 3c). For the  $f$  estimation, a series of lattice fringe images of the particle core are transformed to FFT patterns to obtain the azimuthal intensity of distribution,  $I(\theta)$ , where  $\theta$  is the azimuthal angle between one lattice fringe orientation and a reference axis.<sup>[17]</sup> Then  $f$  can be related to the mean squared cosine of  $\theta$ , as described in Equation (1)

$$f = \frac{3\langle \cos^2 \theta \rangle - 1}{2} \quad (1)$$

$$\text{where } \langle \cos^2 \theta \rangle = \frac{\int_0^\pi \cos^2 \theta \cdot \Delta I(\theta) \cdot \sin \theta d\theta}{\int_0^\pi \Delta I(\theta) \cdot \sin \theta d\theta} \quad (2)$$

For single crystal,  $f = 1$ , and small value of  $f$  indicates poorly crystallized particles. In our experiment,  $f$  of the resulted

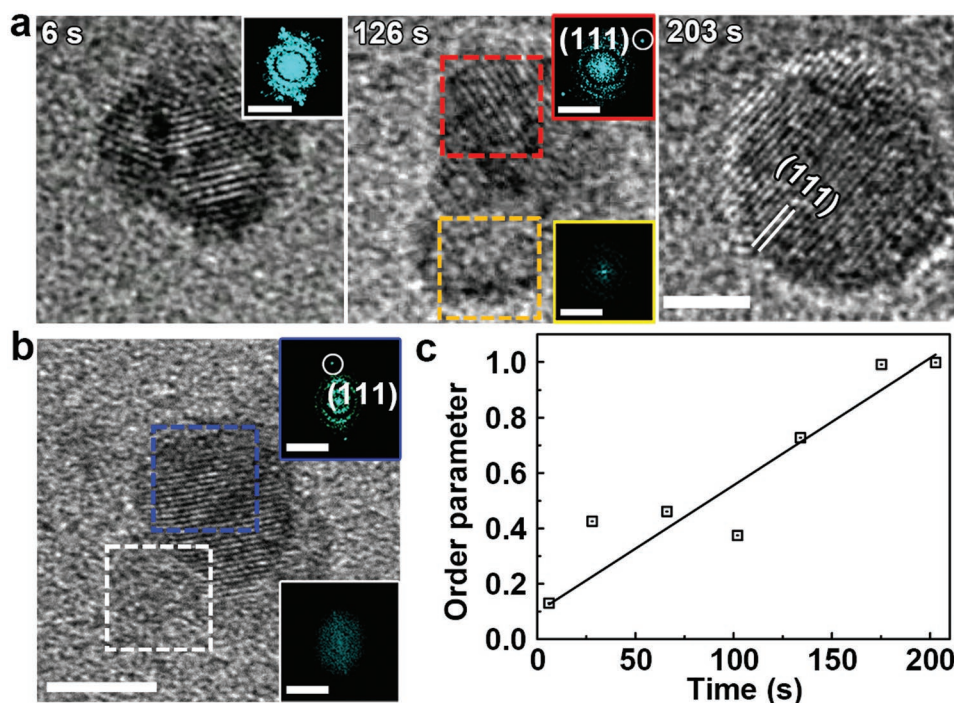


**Figure 3.** The relaxation process of a poorly crystallized Pd nanoparticle to a single crystal. a) Sequential high-resolution TEM and the corresponding FFT images, showing that the nanoparticle evolves from a polycrystal to a single crystal by “out” and “in” processes. Scale bar, 2 nm. b) Ex situ TEM experiment confirms that the degree of crystallinity of the core is higher than cluster-cloud. Scale bar, 5 nm. Scale bar in the FFT images is 5 1/nm. c) The order parameter changes during the relaxation process.



nanoparticles kept increasing from 0.13 to 1.0 (Figure 3c) during the repeated out-and-in relaxation, confirming the maturation from a poorly ordered polycrystalline nanoparticle to a well-defined single crystal by these cluster-cloud mediated out-and-in relaxations.

In order to further consolidate our findings, we performed systematic studies to exclude any possible effects of the electron beam on the multistep nucleation process. First, the out-and-in relaxation process was captured at a reduced electron dose rate of 81 electrons ( $\text{\AA}^2 \text{s}^{-1}$ ) (Figure S11, Supporting Information); and in fact even with no electron beam irradiation at all (Figure S12, Supporting Information). Second, the polycrystal almost kept unchanged when placed on a  $\text{Si}_3\text{N}_4$  membrane or a carbon film and then irradiated by focused electron beam (Figure S13, Supporting Information), proving that the electron beam itself could not induce the relaxation. Third, the electron knock-on effect related to surface atom diffusion<sup>[18]</sup> was expected to be neglectable in this cluster-cloud mediated relaxation process, confirmed by our characterizations under similar conditions (Figure S13, Supporting Information). In addition, the electron beam induced temperature increase in the relaxation process should be of no significance, since from both the calculation (Figure S14, Supporting Information) and literature,<sup>[5a]</sup> we found that the temperature rise was only a few degrees. Last but not least, our ex situ characterizations account for an internally ordered and externally disordered structure of multiple Pd nanoparticles synthesized in flask (Figures S15 and S16, Supporting Information), presumably corresponding to the core-cloud structure captured under LC-TEM (Figure 2c). The above experimental evidence shows that the cluster-cloud mediated nanoparticle crystallization is independent of the

electron beam irradiation and is a universal phenomenon in nanocrystallization.

The cluster-cloud mediated crystallization revealed by our LC-TEM is far from any current knowledge.<sup>[3a,b]</sup> This phenomenon represents a new crystallization pathway, despite the fact that it is not very clear under what specific conditions the cluster-cloud mediated processes would dominate. We speculated that the formation of cluster-cloud was initiated by the fast reduction of precursor and the cluster-cloud was readily to be condensed into the nanoparticle due to its instability. Accordingly, the clusters separation and aggregation may be responsible for the observed out-and-in relaxation.

To complement the experimental characterizations, MD simulations were performed (see Method in the Supporting Information) to gain in-depth understanding of the prenucleation stage and the subsequent grain refinement for providing valuable information at the molecular level. As shown in Figure 4a, during an extended MD simulation period, one Pd nanocluster surrounded by water molecules maintained its original state. Interestingly, when the Pd atoms were initially randomly dispersed in water, the amorphous state formed by those atoms could also be reasonably preserved for the whole simulation time of 30 ns (Figure 4b). This result suggests that the hydration stabilization, applying to both the nanocluster and amorphous Pd, plays a key role in the formation of the cluster-cloud. Figure 4b shows that while the Pd atoms were stabilized by water, they still tended toward aggregation, which is consistent with the experimental observation under LC-TEM (Figure 1a). To quantify the tendency of this aggregation, the radial distribution function (RDF) was calculated (Figure 4c). Examining the RDF for the monocrystalline nanoparticle

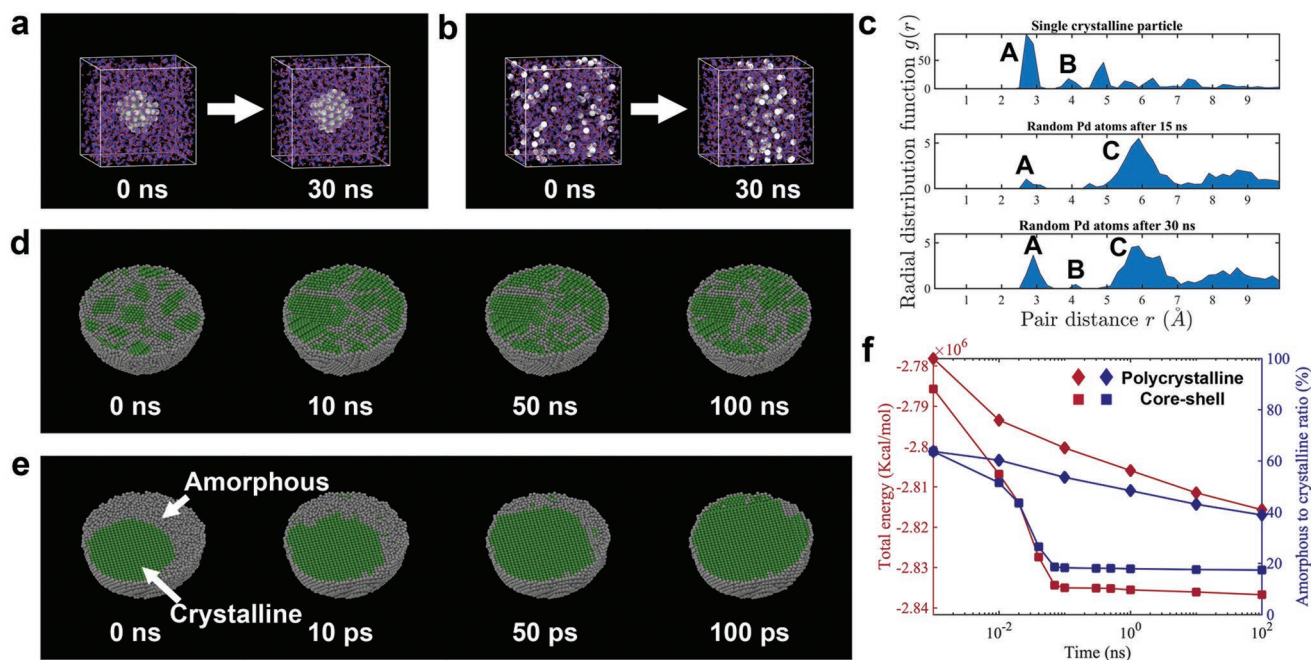


**Figure 4.** Molecular dynamics simulations. a) Snapshots from one simulation of a Pd nanoparticle in water. b) Snapshots from one simulation of randomly distributed Pd atoms in water. c) Radial distribution functions for the Pd-water system. d) The evolution process of a poorly crystallized particle. e) The evolution process of a crystalline core/amorphous shell particle. f) Total energy and amorphous to crystalline ratio plotted as a function of time.

(Figure 4c top), the first two peaks on the left (Peak A and B) correspond to the nearest and the second nearest neighbor Pd atoms, respectively. For the amorphous case (Figure 4c middle and bottom), after a 15 ns simulation, the intensity of peak A was very low, while peak B almost disappeared. On the other hand, a much more pronounced peak at around 6 Å (Peak C) appeared, referring to the clustering of the solvated Pd atoms. Furthering the simulation for another 15 ns, both Peak A and B increased with a slight reduction of Peak C. This result suggests a possible evolution from the collection of solvated Pd atoms to sub-nanometer sized clusters. It confirms that given enough time, Pd atoms can coalesce from a scatter of water-stabilized state into a condensed cluster-cloud complex.

Besides the prenucleation process, MD simulations were also employed to understand the out-and-in relaxations. For simplicity, here we ignored the water molecules, and assumed the initial cluster-cloud configuration as a poorly-crystallized particle (a mixture of amorphous atomic clusters and randomly embedded nanocrystals, as shown in Figure 4d: 0 ns). A series of snapshots are recorded in Figure 4d for a MD simulation with a time span of 100 ns at 300 K. At the end of the simulation, though in average the quality of the grains was improved, the system remained polycrystalline. In comparison, when the system temperature was increased to 800 K to mimic sintering condition, much finer grains could be observed (Figure S17, Supporting Information). This indicates a relatively high activation energy for the conventional local rearrangement pathway such as by dislocation and grain-boundary migration.<sup>[17,19]</sup> As a result, the kinetics were limited for the poorly crystallized particle to evolve to a monocrystalline state at room temperature, at least in a simulation-reachable time scale. Alternatively, an out-and-in relaxation might serve as a kinetically preferred approach. In the “out” process, the Pd nanoparticle (Figure 4d, 0 ns) first evolved into a crystalline core/amorphous shell-like intermediate structure by a spontaneous phase separation of ordered and disordered/amorphous phases (Figure 2), which was speculated to be a rapid aggregation of the grains within the particle.<sup>[3a,20]</sup> Thermodynamically, this process can be promoted by the intergrain Van der Waals forces.<sup>[20]</sup> Kinetically, the diffusivities of both the crystalline and amorphous phases were found to be enhanced in solution (Figure S18, Supporting Information), granting a high mobility of the system for a global rearrangement (out process). Also, when the nanoparticle condensed from the cluster-cloud complex, the collision frequency among the nanograins increased, leading to a greater probability for aggregation.<sup>[21]</sup> With the above discussion regarding the “out” process, we created a core-shell nanoparticle initial configuration (Figure 4e: 0 ns) based on the TEM images in Figure 2a, to study the subsequent “in” process in MD. As shown in Figure 4e, starting with the same amorphous to crystalline (A/C) ratio, the core-shell nanoparticle quickly evolved toward monocrystallinity. In Figure 4f, the A/C ratio and the total energy change in this process were tracked and plotted, in conjunction with the same plots for the polycrystalline simulation. For the core-shell case (data points marked by squares), consistent with Figure 4e, both the A/C ratio and the total energy dropped significantly in a very short period of time at the beginning, and was followed by a slow perfection of the nanocrystal (mostly occurring at the surface) till the end of the simulation. In contrast, the refining of a

polycrystalline particle by local atomic rearrangement, shown as the curves connected by the diamond markers on Figure 4f, was extremely slow and could not be completed within this 100 ns MD simulation period.

In summary, our observations reveal three fundamental steps during nanoparticle crystallization: formation of a cluster-cloud from supersaturated solution (prenucleation), condensation of the cluster-cloud to form a poorly crystallized nanoparticle (nucleation), and multiple out-and-in relaxations toward a well-crystallized nanoparticle (maturation). An intermediate state of condensed atomic clusters (cluster-cloud) and its out-and-in relaxation for nanoparticle maturation are identified for nanocrystallization, which reflects the diverse nature of crystallization pathways, and suggests a new mechanism that has not been described in any previous study. Our findings expand current understanding of nonclassical crystallization theory and can also be developed as an alternative strategy for the design and synthesis of nanostructured material.

## Supporting Information

Supporting Information is available from the Wiley Online Library or from the author.

## Acknowledgements

This work was financially supported by the National Natural Science Foundation of China (21625105, 51772265, and 61721005), the Zhejiang Provincial Natural Science Foundation (D19E020002) and China Postdoctoral Science Foundation (2017M621909). The experiments of electron microscopy were done at the Center of Electron Microscopy of Zhejiang University. The computation resource was provided by National Energy Research Scientific Computing Center (NERSC).

## Conflict of Interest

The authors declare no conflict of interest.

## Keywords

cluster-cloud, crystallization, LC-TEM, nanoparticle, out-and-in relaxation

Received: December 21, 2018

Revised: February 21, 2019

Published online:

- [1] a) R. B. Zhao, X. Y. Liu, X. Y. Yang, B. Jin, C. Y. Shao, W. J. Kang, R. K. Tang, *Adv. Mater.* **2018**, *30*, 1801304; b) Z. X. Fan, H. Zhang, *Acc. Chem. Res.* **2016**, *49*, 2841; c) S. Gwo, H. Y. Chen, M. H. Lin, L. Y. Sun, X. Q. Li, *Chem. Soc. Rev.* **2016**, *45*, 5672.
- [2] a) Y. Z. Lu, W. Chen, *Chem. Soc. Rev.* **2012**, *41*, 3594; b) P. N. Zhang, C. X. Xi, C. Feng, H. B. Xia, D. Y. Wang, X. T. Tao, *CrystEngComm* **2014**, *16*, 5268; c) J. Park, J. Joo, S. G. Kwon, Y. Jang, T. Hyeon, *Angew. Chem. Int. Ed.* **2007**, *46*, 4630; d) B. Lim, Y. N. Xia, *Angew. Chem. Int. Ed.* **2011**, *50*, 76.
- [3] a) J. Lee, J. Yang, S. G. Kwon, T. Hyeon, *Nat. Rev. Mater.* **2016**, *1*, 16034; b) S. Karthika, T. K. Radhakrishnan, P. Kalaiichelvi,

- Cryst. Growth Des.* **2016**, *16*, 6663; c) M. Sleutel, J. Lutsko, A. E. S. Van Driessche, M. A. Duran-Olivencia, D. Maes, *Nat. Commun.* **2014**, *5*, 5598.
- [4] a) C. M. Volkle, D. Gebauer, H. Cölfen, *Faraday Discuss.* **2015**, *179*, 59; b) M. Kellermeier, D. Gebauer, E. Melero-Garcia, M. Drechsler, Y. Talmon, L. Kienle, H. Colfen, J. M. Garcia-Ruiz, W. Kunz, *Adv. Funct. Mater.* **2012**, *22*, 4301; c) S. Chattopadhyay, D. Erdemir, J. M. B. Evans, J. Ilavsky, H. Amenitsch, C. U. Segre, A. S. Myerson, *Cryst. Growth Des.* **2005**, *5*, 523.
- [5] a) N. D. Loh, S. Sen, M. Bosman, S. F. Tan, J. Zhong, C. A. Nijhuis, P. Král, P. Matsudaira, U. Mirsaidov, *Nat. Chem.* **2016**, *9*, 77; b) H. Q. Zhan, X. F. Yang, C. M. Wang, J. Chen, Y. P. Wen, C. L. Liang, H. F. Greer, M. M. Wu, W. Z. Zhou, *Cryst. Growth Des.* **2012**, *12*, 1247; c) T. H. Zhang, X. Y. Liu, *J. Am. Chem. Soc.* **2007**, *129*, 13520.
- [6] a) P. J. Smeets, K. R. Cho, R. G. Kempen, N. A. J. M. Sommerdijk, J. J. De Yoreo, *Nat. Mater.* **2015**, *14*, 394; b) S. Q. Jiang, H. H. Pan, Y. Chen, X. R. Xu, R. K. Tang, *Faraday Discuss.* **2015**, *179*, 451; c) J. Yang, J. Koo, S. Kim, S. Jeon, B. K. Choi, S. Kwon, J. Kim, B. H. Kim, W. C. Lee, W. B. Lee, H. Lee, T. Hyeon, P. Ercius, J. Par, *J. Am. Chem. Soc.* **2019**, *141*, 763.
- [7] M. Y. Liu, K. Wang, L. X. Wang, S. Han, H. S. Fan, N. Rowell, J. A. Ripmeester, R. Renoud, F. G. Bian, J. R. Zeng, K. Yu, *Nat. Commun.* **2017**, *8*, 15467.
- [8] a) F. J. Zhang, F. Roosen-Runge, A. Sauter, R. Roth, M. W. A. Skoda, R. M. J. Jacobs, M. Sztucki, F. Schreiber, *Faraday Discuss.* **2012**, *159*, 313; b) M. A. Bewernitz, D. Gebauer, J. Long, H. Cölfen, L. B. Gower, *Faraday Discuss.* **2012**, *159*, 291; c) O. Galkin, K. Chen, R. L. Nagel, R. E. Hirsch, P. G. Vekilov, *Proc. Natl. Acad. Sci. USA* **2002**, *99*, 8479.
- [9] a) D. Gebauer, M. Kellermeier, J. D. Gale, L. Bergstrom, H. Cölfen, *Chem. Soc. Rev.* **2014**, *43*, 2348; b) R. Demichelis, P. Raiteri, J. D. Gale, D. Quigley, D. Gebauer, *Nat. Commun.* **2011**, *2*, 590.
- [10] a) T. H. Zhang, X. Y. Liu, *J. Phys. Chem. B* **2007**, *111*, 14001; b) P. G. Vekilov, *Nanoscale* **2010**, *2*, 2346; c) M. O. M. Piepenbrock, T. Stirner, M. O'Neill, S. M. Kelly, *J. Am. Chem. Soc.* **2007**, *129*, 7674; d) L. F. Fei, X. L. Gan, S. M. Ng, H. Wang, M. Xu, W. Lu, Y. Zhou, C. W. Leung, C. L. Mak, Y. Wang, *ACS Nano* **2019**, *13*, 681.
- [11] a) W. J. E. M. Habraken, J. H. Tao, L. J. Brylka, H. Friedrich, L. Bertinetti, A. S. Schenk, A. Verch, V. Dmitrovic, P. H. H. Bomans, P. M. Frederik, J. Laven, P. van der Schoot, B. Aichmayer, G. de With, J. J. DeYoreo, N. A. J. M. Sommerdijk, *Nat. Commun.* **2013**, *4*, 1507; b) D. Gebauer, P. Raiteri, J. D. Gale, H. Cölfen, *Am. J. Sci.* **2018**, *318*, 969.
- [12] F. M. Ross, *Liquid Cell Electron Microscopy*, Cambridge University Press, Cambridge **2016**.
- [13] G. M. Zhu, Y. Y. Jiang, F. Lin, H. Zhang, C. H. Jin, J. Yuan, D. R. Yang, Z. Zhang, *Chem. Commun.* **2014**, *67*, 9447.
- [14] a) B. Jin, M. L. Sushko, Z. M. Liu, C. H. Jin, R. K. Tang, *Nano Lett.* **2018**, *18*, 6551; b) Z. Aabdin, J. Lu, X. Zhu, U. Anand, N. D. Loh, H. Su, U. Mirsaidov, *Nano Lett.* **2014**, *14*, 6639; c) U. Anand, J. Lu, D. Loh, Z. Aabdin, U. Mirsaidov, *Nano Lett.* **2016**, *16*, 786.
- [15] A. Leyva-Perez, J. Oliver-Meseguer, P. Rubio-Marques, A. Corma, *Angew. Chem. Int. Ed.* **2013**, *52*, 11554.
- [16] S. Park, K. Schulten, *J. Chem. Phys.* **2004**, *120*, 5946.
- [17] Z. M. Liu, H. H. Pan, G. X. Zhu, Y. L. Li, J. H. Tao, B. Jin, R. K. Tang, *Angew. Chem. Int. Ed.* **2016**, *55*, 12836.
- [18] D. T. Spreng, J. E. Hilliard, J. W. Kauffman, *J. Appl. Phys.* **1972**, *43*, 2040.
- [19] S. A. Hackney, F. S. Biancaniello, D. N. Yoon, C. A. Handwerker, *Scr. Metall. Mater.* **1986**, *20*, 937.
- [20] F. Wang, V. N. Richards, S. P. Shields, W. E. Buhro, *Chem. Mater.* **2013**, *26*, 5.
- [21] D. L. Van Hying, W. G. Klemperer, C. F. Zukoski, *Langmuir* **2001**, *17*, 3128.